Final Technical Report on NCC 2-666: Counting Particles Emitted by Stratospheric Aircraft and Measuring Size of Particles Emitted by Stratospheric Aircraft

Report Covering Time Period:
01 May 1990 to 31 December 1992

Submitted by James Charles Wilson
Principal Investigator
Department of Engineering
University of Denver
Denver, CO 80208

April 19, 1994

Objectives of the Cooperative Agreement

There were two principal objectives of the cooperative agreement between NASA and the University of Denver. The first goal was to modify the design of the ER-2 condensation nuclei counter (CNC) so that the effective lower detection limit would be improved at high altitudes. This improvement was sought because, in the instrument used prior to 1993, diffusion losses prevented the smallest detectable particles from reaching the detection volume of the instrument during operation at low pressure. Therefore, in spite of the sensor's ability to detect particles as small as 0.008 microns in diameter, many of these particles were lost in transport to the sensing region and were not counted.

Most of the particles emitted by aircraft are smaller than 0.1 μm in diameter. At the start date of this work, May 1990, continuous sizing techniques available on the ER-2 were only capable of detecting particles larger than 0.17 micron. Thus, the second objective of this work was to evaluate candidate sizing techniques in an effort to gain additional information concerning the size of particles emitted by aircraft.

Accomplishments during this Cooperative Agreement

Redesign of the ER-2 CNC. The design of the ER-2 CNC was evaluated under this grant and revisions were made in the design which would permit a larger fraction of small particles to reach the detection volume of the instrument during low pressure operation. These design changes were implemented in the construction of the ER-2 CNC II which was used in the 1993 Stratospheric Photochemistry, Aerosol and Dynamics Expedition and in ASHOE/MAESA flights which are currently under way. Figure 1 shows the design changes incorporated into the ER-2 CNC as a result of this work. The redesigned instrument, the ER-2 CNC II, was constructed with support from another grant. The response of the current, redesigned CNC is less dependent on pressure than that of the previous instrument.

Evaluation of sizing techniques. A number of techniques were evaluated for determining the sizes of particles smaller than 0.1 micron in diameter. These techniques included a differential mobility analyzer (DMA) and a diffusion battery (DB). In addition, the possibility of extending the lower size range of the optical particle counter was also considered. The object was to provide accurate size distributions of particles emitted from aircraft flying in the stratosphere.

Evaluation of the DMA technique

Technical reports generated in the study of the DMA are attached in Appendices 1 and 2. A summary of the results is given here.

The DMA technique promises high resolution measurements of aerosol size distributions. The technique consists of exposing the aerosol to a bipolar ion atmosphere which will

neutralize most of the particles but leave a certain number with a single charge, fewer with a double charge, etc. After this conditioning, the aerosol is introduced into the DMA where particles are exposed to known flow and electric fields. These fields are crossed so that only particles within a narrow range of electrical mobilities can reach the exit region. Thus, ignoring the effects of multiple charging, particles within a very narrow size range--virtually monodisperse--exit the DMA. These particles are counted by a CNC. By varying the voltage and/or the flow, a spectrum particle concentration vs. particle mobility may be measured. Accounting for multiple charging effects, this spectrum can be converted to a size distribution for particles larger than the CNC detection limit (about 0.008 μm diameter). Thus, this technique hold the promise of high-resolution size distribution measurements of particles in the size range likely to be produced by jet engines.

The analysis of the DMA alternative in Appendices 1 and 2 shows that there are two fundamental issues which remain unresolved for a stratospheric DMA. The first issue involves the effects of Brownian diffusion on the transfer function of the DMA. Discrepancies between the predicted and actual transfer function for very small particles--those most affected by diffusion--exist in the literature. These discrepancies suggests that the effects of diffusion are not precisely predictable or experimentally controllable. Since diffusion is increasingly important as pressure decreases, the response of a stratospheric DMA may not be fully predictable. The magnitude of this effect has not been ascertained.

A second problem associated with the operation of the DMA at stratospheric pressures involves the charging of aerosol at low pressure (Appendix 2). The recovery of a size distribution from a DMA depends critically on the distribution of charges on aerosol particles resulting from the ion preconditioning process. Although ion properties and aerosol chargeing have been studied at atmospheric pressure, there is little literature on these processes at low pressure. It may be possible to use the preexisting ambient charge distribution and avoid the the artificial preconditioning problem. At the current time, the knowledge of stratospheric ion concentrations, ion-attachment coefficients at low pressure, and the charge distribution on particles found in aircraft exhaust is insufficient to evaluate the effectiveness of a stratospheric DMA.

A third problem involving a stratospheric DMA, one not discussed in the appendix, is associated with the absolute concentration of particles available in the stratosphere. Only a small fraction of the particles upstream of the DMA are charged in the preconditioning process. Since the concentration of stratospheric particles is quite small, obtaining a reasonably accurate size distribution measurement in the stratosphere would require extremely long sampling times to obtain a statistically significant signal. The aerosol being measured would have to remain relatively constant over the long measuring time. Even in the plume of an aircraft, the large spatial variations in particle concentrations would make complete particle size measurements with a DMA impractical.

Given the uncertainties in diffusion losses within a DMA at low pressure, the unknown distribution of charges on stratospheric particles, and the low concentrations of these

particles that imply very long sampling times, using a DMA for measuring stratospheric aerosol size distributions appears to be impractical. Some of these uncertainties may be reolved with future laboratory measurements and modelling studies; however, the problem of long sampling times will probably require fundamental changes in DMA design and may remain unsolved.

Evaluation of diffusion battery technique

Diffusion batteries have been used for decades to evaluate the size distribution of small particles in the atmosphere. In this class of instruments, particles are separated by passing the aerosol through a "battery" of screens or tube arrays. Particles with high diffusional mobilities (i.e., small particles) diffuse to the walls of the battery and are removed from the airstream. The remaining particles are counted by a CNC.

There are several problems associated with determining particle size distributions from diffusion batterie measurements. The main difficulty lies in the nature of the response function and the difficulty in recovering accurate particle size distributions from the response function. These difficulties are discussed in more detail in Appendix 3. Briefly, the diffusion battery does not provide a sharp discrimination of particle size, rather a very gradual one. The measured parameters are strongly convoluted with the response function and must be deconvolved, or inverted, to obtain the original distribution. Because this convolution is of the form of a Fredholm integral equation of the first kind, there are an infinity of possible solutions (particle size distributions) that could produce the measured response. Various techniques are availabe that constrain the equation and produce the "best" solution, while another reports all physically possible solutions, giving a wide range of particle size distributions. When measurement errors are added to the inversion, the recovery of a particle size distributions becomes very difficult. Because of these problems, DMAs are diffusion batteries are rarely used now in cases where a DMA can be applied.

Because of the fundamental problems associated with inverting diffusion battery data and recovering a size distribution, it is unlikely the diffusion batteries can be used to evaluate the details of the size distribution of small particles in the stratosphere. However, the technique shows some limited promise in providing rough estimates of some important parameters--such as mean particle size--in the diameter range from 0.008 to 0.1 μm.

Redesign of the PMS aerosol spectrometer

In response to requests made by Dr. Guy Ferry of NASA Ames Research Center, Particle Measuring Systems Inc. (PMS, Boulder, CO) offered to build an optical particle counter capable of sizing particles as small as 0.05 μm in diameter. Since the instrument heats particles before measuring them and thus reduces their size, a sulfuric acid particle having a diameter of 0.05 μm at the laser would have a diameter approaching 0.07 μm under ambient temperatures and water vapor mixing ratios. This instrument, the focused-cavity aerosol spectrometer, or FCAS, represents a considerable advance on the previous model,

the active-scattering aerosol spectrometer. NASA has purchased the upgraded optical particle counter. The FCAS flew successfully on the AASE-II and SPADE missions before being replaced with a model with an improved laser and new pulse analysis hardware. The FCAS instruments have collected data that indicate the presence of a mode of small particles when the CNC counts high concentrations of particles, although this mode is only partially resolved by the spectrometer measurements.

Summary

The ER-2 CNC has been modified to reduce the diffusive losses of particles within the instrument. These changes have been successful in improving the counting efficiency of small particles at low pressures.

Two techniques for measuring the size distributions of particles with diameters < 0.17 μm have been evaluated. Both of these methods, the DMA and the diffusion battery, have fundamental problems that limit their usefulness for stratospheric applications. We cannot recommend either for this application. Newly developed, alternative methods for measuring small particles include inertial separation with a low-loss critical orifice and thin-plate impactor device. This technique is now used to collect particles in the multi-sample aerosol collector housed in the ER-2 CNC-II, and shows some promise for particle size measurement when coupled with a CNC as a counting device.

The modified FCAS can determine the size distribution of particles with ambient diameters as small as about 0.07 μm. Data from this instrument indicate the presence of a nuclei mode when the CNC-II indicates high concentrations of particles, but cannot resolve important parameters of the distribution.

Bibliography.

No publications resulted from these engineering and feasibility studies.

Figure Captions:
Figure 1. Assembly A shows the design of the ER-2 CNC. In this instrument, the sample was drawn through the sample flow meter, A1, up the injector in the vertical saturator, A2, and into the condenser. In the revised design, Assembly B, the flow meter and injector are combined which leads to a shorter length from the inlet to the saturator. Thus fewer particles are lost by diffusion.

Figure 2. Modelled response function of a tube-array diffusion battery under stratospheric conditions.

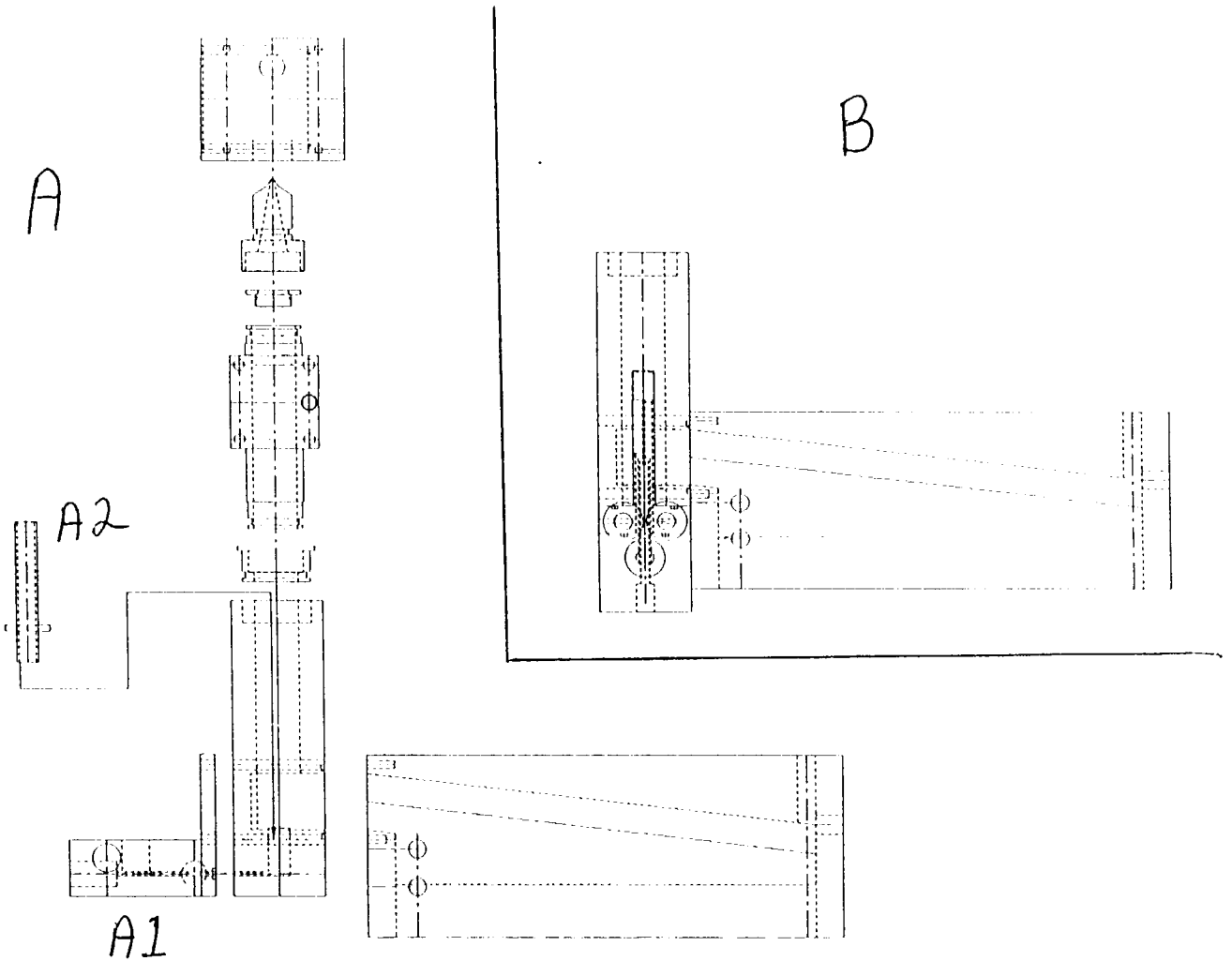

Figure 1. Assembly A shows the design of the ER-2 CNC. In this instrument, the sample was drawn through the sample flow meter, A1, up the injector in the vertical saturator, A2, and into the condenser. In the revised design, Assembly B, the flow meter and injector are combined which leads to a shorter length from the inlet to the saturator. Thus fewer particles are lost by diffusion.

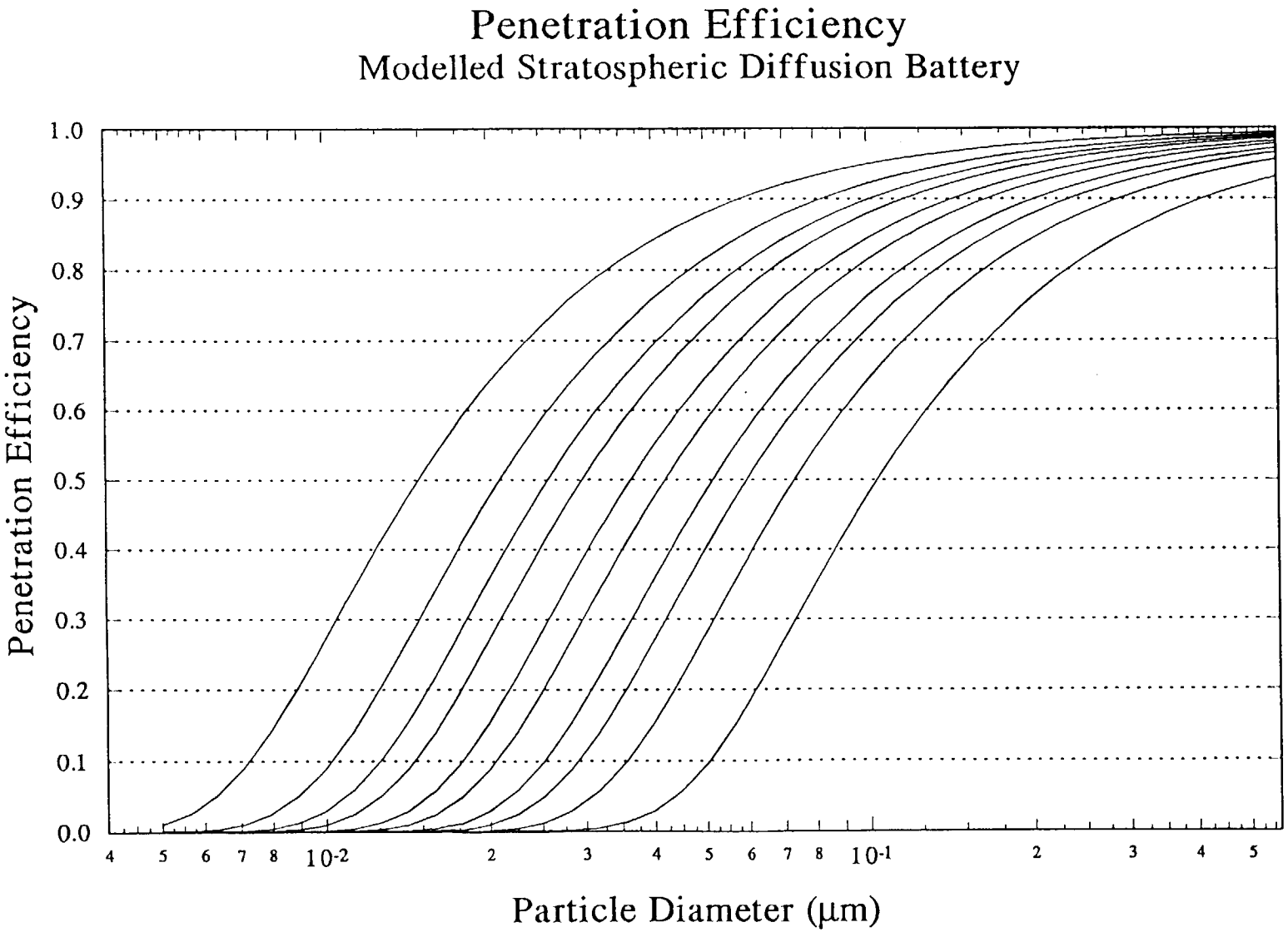

Figure 2. Modelled response function of a tube-array diffusion battery under stratospheric conditions.

Appendix 1

STRATOSPHERIC DMA

NOMENCLATURE

Dimensional variables:

t = time

r = radial coordinate

z = axial coordinate

$\vec{u}$ = flow velocity at r,z

$\vec{E}$ = electric field at r,z at time t

V = analyzer voltage at time t

Dimensional parameters:

Z_p = particle electric mobility

D = particle diffusivity

R_1 = radius of central rod

R_2 = inner radius of outer cylinder

$D_h = 2(R_2-R_1)$ = hydraulic diameter

L = axial distance between aerosol entrance and exit slits

Δz_a = axial width of aerosol entrance slit

Δz_s = axial width of aerosol exit slit

Q_a = aerosol entrance flow

Q_s = aerosol exit flow

Q_c = sheath entrance flow

Q_m = sheath exit flow

$Q_t = Q_a+Q_c = Q_s+Q_m$ = total flow

$U = Q_t/\pi(R_2^2-R_1^2)$ = mean flow velocity

V_0 = analyzer voltage at t=0

τ = analyzer voltage scan time constant

$Z_p^* = (Q_m+Q_c)\cdot\log(R_1/R_2)/4\pi LV$ = centroid of steady-state transfer function at V

$Z_{p0}^* = Z_p^*(V=V_0)$

Dimensionless variables:

$\tilde{t} = t/\tau$

$\omega = (r/R_2)^2$

$\tilde{z} = z/D_h$

Dimensionless parameters:

$\gamma = (R_1/R_2)^2$

$\kappa = LR_2/(R_2^2-R_1^2)$

$\kappa_a = \Delta z_a/L$

$\kappa_s = \Delta z_s/L$

$\beta = (Q_s+Q_a)/(Q_m+Q_c)$

$\delta = (Q_s-Q_a)/(Q_s+Q_a)$

G = geometric flow factor

$\tilde{D} = 4\pi LD/(Q_m+Q_c)$

$\sigma^2 = G\cdot\tilde{D}$

$\sigma^{*2} = \sigma^2(Z_p=Z_p^*) = G\cdot\tilde{D}^*$

$Re = \rho UD_h/\mu$ = Reynolds number

$S = L/\tau U$

$\tilde{Z}_p = Z_p/Z_{p0}^*$

INTRODUCTION

It is proposed to develop a new particle sizing system to be operated aboard the ER–2 in the stratosphere. One of the possible measurement systems consists of a differential mobility analyzer (DMA) operated upstream of a condensation nucleus counter (CNC). The purpose of the DMA is to extract aerosol within a known narrow size range and present it to the CNC for concentration measurement. The response of the DMA is well understood in its standard steady-state mode (Knutson and Whitby, 1975a). However, for this project it proposed to operate in the scanning mode described by Wang and Flagen (1990). Use of the scanning mode may present several problems depending on the rate of scan. Some of these problems may be confounded by particle Brownian diffusion which is significant for the proposed application. Aerosol charging is also a major area of uncertainty.

In the discussion below, the DMA scanning mode is first analyzed neglecting diffusion. Diffusion effects are discussed in the following section. Aerosol charging is discussed in a separate paper.

SCANNING MODE AND CHARACTERISTIC TIMES

Strictly laminar flow may be assumed within the DMA classification section itself. In general, laminar flow may be assumed from some indeterminate point upstream of the DMA all the way to the CNC viewing volume. There may be some mixing at certain points in the transport lines, such as just inside the DMA aerosol exit slit, which will affect the following analysis. But for the most part, particles may be assumed to follow flow streamlines in the absence of diffusion and the DMA electric field.

In analyzing the transit of a particle through the proposed measurement system, there are several key locations along its trajectory from the sample point to the detector. The first is where it enters the sampling system at the tip of the external sample probe, designated as p. Well mixed flow is assumed from p to b, the point where laminar flow begins upstream of the DMA. The DMA aerosol entrance and exit slits are designated as a and s, respectively, the CNC detection volume as d. Let τ_m represent the average particle transit time through the well mixed zone from p to b. Let τ_a, τ_x and τ_s represent the average particle transit times from b to a, a to s, and s to d, respectively. Let t_p, t_b, t_a, t_s, and t_d represent the times at which a particular particle passes the respective points. An inherent assumption for the well mixed zone is that all particle transit times are the same, *i.e.* $t_b - t_p = \tau_m$. But for the laminar flow regions the transit times for a particular particle depend on which streamline it is on. Because of slow flow near walls, the variation of transit times through the laminar zones upstream and downstream of the DMA is on the order of the mean transit times, τ_a and τ_s. The variation of transit time through the DMA itself is significantly less than τ_x. Let τ represent the period over which the voltage of the scanning DMA changes by a significant amount, and τ_f the period over which the ambient aerosol size distribution changes by a significant amount. The CNC sample interval is designated as τ_d.

Even when operated in the steady-state mode, the size range extracted by the DMA has a finite width determined by the ratio of aerosol to sheath flows. When operated in the scanning mode there are several factors acting to broaden the particle size range presented to the CNC at any given instant.

Particles arriving at the CNC at a given instant have exited the DMA at point s over a range of earlier times. If $\tau_s << \tau$ does not hold, then the mean particle size exiting the DMA has changed significantly over this time range resulting in a broadening of the

size range presented to the CNC at that instant.

If $\tau_x << \tau$, then the DMA voltage may be treated as constant over the period of a single transit of the DMA classification section and there is no broadening of the extraction range for this part of the particle trajectory. However, as the scan rate is increased (τ decreased) the DMA transfer function is increasingly warped from its basic triangular shape and becomes broadened. (See results of SCAN simulation program.)

If $\tau_d << \tau$ does not hold, then again the particle size exiting the DMA has changed significantly over the sample interval resulting in broadening of the effective average extraction range over the interval.

For normal stratospheric sampling τ_f may be assumed to be large compared to the sampling system transit time. This condition may be strained somewhat for the High Speed Research Program when flying through a fresh jet plume. If the laminar flow zone transit time is not small compared to τ_f then particles arriving at the CNC at a given instant have been sampled from the ambient over a range of times during which the ambient size distribution has changed significantly.

In general, if τ and τ_f are large compared to τ_a, τ_x, τ_s and τ_d then the measurements can be treated as steady-state. If $\tau >> \tau_d$ does not hold, then the response of the measurement system is still relatively easy to analyze in terms of an average size extraction range over the sample period. If τ is not large compared to τ_a, τ_x or τ_s then the problem becomes much more difficult. Particle diffusion makes theoretical analysis of the effect of transit time variation extremely difficult.

DMA TRANSFER FUNCTION IN SCANNING MODE

Consider a particle traversing the classifier from the aerosol entrance slit to the aerosol exit slit. It starts at radial position $\omega=1$ on a streamline designated by $\tilde{Q}_{in}$ and ends at radial position $\omega=\gamma$ on a streamline designated by $\tilde{Q}_{out}$. $\tilde{Q}_{in}$ and $\tilde{Q}_{out}$ are proportional to stream function. $\tilde{Q}_{in}$ is 0 on the center streamline of Q_a, -1 on the downstream edge of the entrance slit and $+1$ on the upstream edge. $\tilde{Q}_{out}$ is 0 on the center streamline of Q_s, -1 on the downstream edge of the exit slit and $+1$ on the upstream edge. In the steady-state mode, the dimensionless mobility $\tilde{Z}_p$ of a particle traversing from

$(1,\tilde{Q}_{in})$ to $(\gamma,\tilde{Q}_{out})$ does not depend on the flow velocity profile. This is not the case in the scanning mode.

Unless the flow profile can be accurately determined by numerical modeling, the DMA transfer function must be calibrated experimentally. The dimensionless flow velocity profile $\tilde{u}/U$ is a function of position $(\omega,\tilde{z})$ and depends on the dimensionless parameters Re, β, δ, γ, κ, κ_a and κ_s. Calibration is required over the entire range of these parameters anticipated to be encountered under ER–2 flight conditions. For a given DMA, γ, κ, κ_a and κ_s are fixed by geometry. β, δ are determined by the relative values of the DMA flows. If the flow split is kept constant then β, δ remain constant. Re is likely to vary during flight due to the large pressure range covered. A constant mass flow control strategy would be required to keep Re constant. This is difficult in view of issues discussed below.

If the functional time dependence of the scanning DMA voltage is of the form $V=V_0\cdot\exp(t/\tau)$ where τ is positive or negative, then all particles traversing the classifier from $(1,\tilde{Q}_{in})$ to $(\gamma,\tilde{Q}_{out})$ follow the same trajectory. In this case, DMA transfer can be characterized by the function $W=W(\tilde{Q}_{in},\tilde{Q}_{out},S)$ where S is the dimensionless scan rate. If V is not of exponential form then the transfer characteristic depends on particle mobility (size) as well, making experimental calibration much more arduous.

Assuming an exponential form for V, the sensitivity of the transfer characterization function W to the flow profile, hence, to Re, β, δ, γ, κ, κ_a and κ_s, can be estimated by calculating W for several trial profiles. The basic profile used consists of pure axial flow for the bulk of the region between $\omega=1$ and $\omega=\gamma$ except for pure radial flow regions at the aerosol entrance and exit slits connecting streamlines in the entering and exiting aerosol flows to the corresponding streamlines in the axial flow region. Slug and Poiseuille axial profiles were used matched with uniform radial profiles in both cases. A uniform radial electric field was assumed.

Particle trajectories were calculated for the above set of flow and electric fields. A particle entering on streamline $\tilde{Q}_{in}$ at $\omega=\omega_2=1$ follows that streamline radially (at increased velocity due to radial electric field) to radial position $\omega_{in}(\tilde{Q}_{in})$ where it enters the axial flow region. It moves axially due to the flow and radially due to the electric field across fluid streamlines until it reaches streamline $\tilde{Q}_{out}$ at radial position $\omega_{out}(\tilde{Q}_{out})$. It then follows that streamline radially (at increased velocity) to radial position $\omega=\omega_1=\gamma$ where it exits the classification section. ω_{in} and ω_{out} are determined by

$$\tilde{Q}(\omega_{in}) = (1+\tilde{Q}_{in})\beta(1-\delta)/2(1+\beta)$$
$$\tilde{Q}(\omega_{out}) = 1-(1+\tilde{Q}_{out})\beta(1+\delta)/2(1+\beta)$$

where

$$\tilde{Q}(\omega) = \frac{1}{1-\gamma}\cdot\int_{\omega}^{1}\tilde{u}_z(\omega')\,d\omega'$$

is the fraction of total flow between radial position ω and 1, and $\tilde{u}_z(\omega)=u_z/U$ is the dimensionless axial velocity profile.

W is the solution to the equation

$$1=\frac{1}{S}\cdot\int_{\omega_{out}}^{\omega_{in}}\frac{\tilde{u}_z(\omega)}{(W-\omega)}\,d\omega\ .$$

The dimensionless mobility $\tilde{Z}_p$ of the particle traversing the classifier from $(1,\tilde{Q}_{in})$ to $(\gamma,\tilde{Q}_{out})$ and located at radial position $\omega_{in}\geq\omega\geq\omega_{out}$ in the axial flow region at time t is given by

$$W=\omega+\left[\frac{1-\gamma}{1+\beta}\right]\cdot\frac{\tilde{Z}_p}{S}\cdot e^{t/\tau}\ .$$

If t_2, t_{in}, t_{out} and t_1 are the times the particle is at radial positions ω_2, ω_{in}, ω_{out} and ω_1, respectively, then these are related by

$$e^{(t_2-t_{in})/\tau}=\frac{W-\omega_2}{W-\omega_{in}}-\frac{1}{W-\omega_{in}}\cdot\left[\frac{1-\gamma}{\kappa_a}\right]\cdot\left[\frac{\beta(1-\delta)}{1+\beta}\right]\cdot\left[\frac{t_2-t_{in}}{S\tau}\right]$$
$$e^{(t_{out}-t_{in})/\tau}=\frac{W-\omega_{out}}{W-\omega_{in}}$$
$$e^{(t_1-t_{out})/\tau}=\frac{W-\omega_1}{W-\omega_{out}}-\frac{1}{W-\omega_{out}}\cdot\left[\frac{1-\gamma}{\kappa_s}\right]\cdot\left[\frac{\beta(1+\delta)}{1+\beta}\right]\cdot\left[\frac{t_1-t_{out}}{S\tau}\right]\ .$$

Derivations of these equations are given in the handwritten notes.

The DMASCAN Fortran library is intended for use as an extension of the DMA Fortran library which is internally documented. DMASCAN contains the following functions with correspondence to the above notation as noted:

FDENS(T,P) = $\rho(T,p)$
ZSCAN(QIN,QOT,STIM,LPRO,IND,TSCAN) = $[\tilde{Z}_p e^{t_1/\tau}](\tilde{Q}_{in},\tilde{Q}_{out},S,,,(t_1-t_2)/\tau)$
EXPLIN(A,B) = root of e^x+Bx-A
WSCAN(WIN,WOT,GAM,STIM) = $W(\omega_{in},\omega_{out},\gamma,S)$
DSCANL(W,VF) = $[\tilde{u}_z(\omega)\cdot(W-\omega)/S](\omega,\tilde{u}_z)$
WFLOW(F,G) = $\omega(\tilde{Q})$
VFLOW(W,G) = $\tilde{u}_z(\omega,\gamma)$.

The ZSCAN function returns the parameter $\tilde{Z}_p e^{t_1/\tau}$ which can be used to calculate the mobility of a particle which traverses the indicated path and arrives at the exit slit ($\omega=\omega_1$) at time t_1. LPRO is an integer flag indicating the axial flow profile: 0=slug, 2=Poiseuille. LPRO is passed to WFLOW and VFLOW through COMMON block FLOPRO. IND is an integer index referring to DMA configuration parameters stored in COMMON blocks defined by a call to DMASET in the DMA library. These COMMON blocks supply the required values of γ, κ_a, κ_s, β and δ to ZSCAN. ZSCAN uses EXPLIN to solve the transcendental equations for the classifier transit times. The total dimensionless classifier transit time $(t_1-t_2)/\tau$ is returned as an output argument of ZSCAN. WSCAN finds W through a search routine which calls TSIMP, a Simpson numerical integration routine in the DMA library, for which DSCANL calculates the integrand. WFLOW supersedes the DMA library version for applications requiring LPRO=0. For the DMASCAN version to supersede the DMA version in linking, the DMASCAN library must be listed before the DMA library. FDENS is not used by any of the other DMASCAN functions but is used elsewhere for calculating Re. FDENS complements FVISC and FPATH in the DMA library which calculate air viscosity and mean free path.

SCANF and SCAN are applications programs which utilize the DMASCAN library. Both programs are currently set up to give characteristics of the TSI Model 3071 DMA operated in the scanning mode at one atmosphere and 300K with 2 and 20 lpm aerosol and sheath flows. Both routines ask the user for LPRO and S. SCANF also requires $\tilde{Q}_{in}$ and $\tilde{Q}_{out}$ and returns ω_{in}, ω_{out}, W, $\tilde{Z}_p e^{t_1/\tau}$ and $(t_1-t_2)/\tau$. SCAN returns $\tilde{Z}_p e^{t_1/\tau}$ and $(t_1-t_2)/\tau$ for $\tilde{Q}_{in}=0$ and $\tilde{Q}_{out}=0$ and deviations of these parameters for an array of $\tilde{Q}_{in}$ and $\tilde{Q}_{out}$ values specified by the user. The values are printed on the screen and into the file SCAN.DAT. Files of the form PnSx.DAT are sample results of SCAN output.

The actual DMA transfer function Ω as defined in Wang and Flagen (1990) is obtained by some sort of integration of $\tilde{Z}_p e^{t_1/\tau}$ over $\tilde{Q}_{in}$ and $\tilde{Q}_{out}$. This has not yet been derived.

If mixing of the flow streamlines does not occur between the classifier aerosol exit slit and the CNC detection volume, then a rigorous analysis of the effective instantaneous DMA transfer function as seen at the CNC would require taking into account the varying transit time t_d-t_s ($t_s=t_1$) between the DMA and the CNC for each exit streamline $\tilde{Q}_{out}$.

PARTICLE DIFFUSION

Brownian diffusion of particles is an important effect for the proposed measurements of fine and ultrafine aerosols in the stratosphere. The particle diffusion coefficient is independent of pressure in the continuum regime and inversely proportional to pressure in the kinetic (free-molecule) regime. With a mean free path in air (at 23° C) of 0.067 μm at one atmosphere increasing to 1.36 μm at 50 mbar, the aerosol of interest is mostly in the kinetic and transition regimes. Consequently, particle diffusion is of increasing importance in the higher altitude range of the ER–2.

There are two major effects of particle diffusion on the operation of the DMA on the ER–2. The first is particle loss to the walls of sampling and transport lines. For laminar flow these losses can be predicted using the theory of Gormley and Kennedy (1949). The second effect is a broadening of the response function of the DMA. This is due to diffusion within the actual classification section of the DMA and in the transport tube from the DMA aerosol exit slit to the detection volume of the CNC. This second effect is much more difficult to analyze and is also coupled with the loss effect.

Cross-stream diffusion causes particles to travel randomly between adjacent streamlines in the classifier and transport tubes. For a particle entering a transport tube on a given streamline, this leads to a probability distribution of transit times and exit streamlines. The author is not aware of any analytic or even numeric or Monte Carlo solution to this problem. Particle loss to the walls of the transport tube should have some limiting effect on the breadth of this probability distribution. Streamwise diffusion contributes also contributes to the distribution of transit times.

A rigorous analysis of diffusion effects in the classifier is even more difficult. However, Kousaka *et al.* (1985, 1986) and Stolzenburg (1988) have analyzed the problem of diffusion in the steady-state DMA. Kousaka *et al.* have done a dimensional analysis of the problem and show results of an approximate numerical model and experiments. Stolzenburg has constructed an approximate analytic model which is perhaps more convenient for estimating diffusion effects in the stratospheric DMA.

The non-diffusing DMA transfer function $\Omega(\tilde{Z}_p)$ is triangular in shape (Knutson and Whitby, 1975a). As diffusion increases in importance, Ω becomes smaller and broader and more Gaussian in shape. The analytic model of Stolzenburg shows that $[\int \Omega(\tilde{Z}_p) d\tilde{Z}_p]$

remains constant at $\beta(1+\delta)$ while the mean (centroid) and standard deviation of $\Omega(\tilde{Z}_p)$ are given by $1+\sigma^{*2}$ and $[\beta^2(1+\delta^2)/6+\sigma^{*2}(1+\sigma^{*2})]^{1/2}$, respectively. The dimensionless diffusion parameter σ^* is given by $\sigma^{*2}=G\cdot\tilde{D}^*$. $\tilde{D}^*$ is the dimensionless diffusivity of the particle corresponding to $\tilde{Z}_p=1$ and is the same as the parameter $\bar{D}/\bar{E}$ extracted in the dimensional analysis of Kousaka *et al.* (1985). G is a geometric flow factor evaluated as an integral along the particle trajectory. For the TSI Model 3071 with $\beta=1/10$, $\delta=0$ and the same simplified flow field as described above, $G=4.1104$ for Poiseuille flow and $G=3.5110$ for slug flow.

The steady-state analysis of diffusion in the DMA can be used as a first approximation for the diffusion effects in the scanning DMA. As the relative scan rate S increases the error in this approximation also increases. The formulas above for the mean and standard deviation of $\Omega(\tilde{Z}_p)$ can be used to estimate the degree of the diffusion effect. The full form of the steady-state transfer function for diffusing aerosols can obtained and employed in data reduction using the DMA library.

The experimental data obtained by Stolzenburg (1988) to verify his diffusion theory indicate a discrepancy which may be significant for the stratospheric DMA. Figure 4.8 in Stolzenburg (1988) plots the relative error of the theory in predicting the mean mobility extracted by the second DMA in a tandem DMA (TDMA) experiment. Based on the experimental measurements, the theory shows an apparent growth of the aerosol in going from DMA1 to DMA2 when, in fact, there is no physical explanation for such growth. Other investigators have observed this same effect to a lesser degree for larger particle sizes. As seen from the top plot in figure 4.8, the effect increases as particle size decreases. The two experiments at different flow rates indicate that the effect also depends on something other than particle diameter. The lower plot shows a good correlation for both experiments with a measure of the relative broadening of the DMA transfer function due to diffusion. If this correlation is not merely coincidental it may indicate an error in the diffusion model which is proportional to the relative effect of diffusion. Depending on operational parameters, the relative diffusion effect in the stratospheric DMA is likely to extend beyond the range indicated in the lower plot of figure 4.8. Thus, substantial errors could occur in sizing the aerosol if the diffusion theory is in error as suggested.

The experimental data of Stolzenburg indicate that the theory accurately predicts the width (standard deviation) of the transfer function. The discrepancy described above may be due to an unpredicted skewing of the transfer function. There is some ambiguity in

the derivation of the form and use of G in the equations. The programs SCANG, GVAR and FVCOR represent attempts to estimate the magnitude of the effect of these ambiguities on the theory. They indicate that the magnitude is insufficient to explain the discrepancy in the TDMA experiment. The effect of space charge in the TDMA experiment was also analyzed and also appears to be insufficient to explain the discrepancy. Hence, the discrepancy cannot be explained and could be significant for the stratospheric DMA.

The DMASET subroutine in the DMA library evaluates G for the particle trajectory from $\tilde{Q}_{in}$=0 to $\tilde{Q}_{out}$=0 for Poiseuille flow. (Program GCON, not in the library, back calculates G from variables in the DMA COMMON blocks.) The SCANG program, similar to SCAN, calculates G for an array of $\tilde{Q}_{in}$ and $\tilde{Q}_{out}$ values for either slug or Poiseuille flow. Contained within the SCAN.FOR file are functions FGEO and GINT. FGEO calculates G for specified $\tilde{Q}_{in}$ and $\tilde{Q}_{out}$ values, flow profile flag (LPRO) and DMA configuration index (IND). FGEO calls GINT which supersedes the DMA library version for applications requiring LPRO=0.

Appendix 2

AEROSOL CHARGING FOR STRATOSPHERIC DIFFERENTIAL MOBILITY ANALYZER

INTRODUCTION

A major area of uncertainty in reducing data from a differential mobility analyzer (DMA) operated in the stratosphere is the question of the electric charge distribution on the aerosol. In order to obtain the size distribution of all aerosol in the sampled air, it is necessary to know the form of the charge distribution function $f_i^{(k)}(D_p)$, the fraction of particles of diameter D_p carrying k charges of polarity i. This must be calculated for the most part from theory. Several groups have contributed theories and/or experimental data toward this goal. A list of key investigators, one for each group, is: Fuchs, Hoppel, Marlow, Adachi, Pui, Wiedensohler, and Vienna (Porstendörfer *et al.*)

The most promising theory to date for determining ion-aerosol attachment coefficients appears to be that of Fuchs. There seems to be general agreement that Fuchs' theory works well in the continuum regime and well into the transition regime. This is the basis for most of the theoretical work of the groups mentioned above. Hoppel and Marlow have made the greatest efforts to modify Fuchs' theory to obtain better agreement with experimental data in the near free-molecule regime. The best data for making comparisons appears to be that of Adachi, Kousaka and Okuyama (1985) and of Pui, Fruin and McMurry (1988) though the latter is plotted in a much more convenient manner. Adachi compared his results to Fuchs' original theory while Pui compared his results to Fuchs' original theory and to a theory of Marlow. In a subsequent comment on Pui's paper, Marlow and McFarlane (1988) showed improved agreement with Pui's data using a modified theory. In another comment, Hoppel and Frick (1989) showed good agreement of their theory with Pui's data and state (from personal communication with Marlow) that there is an error in Marlow's comment paper. Thus, Fuchs' theory as modified by Hoppel appears to be the best theory to date. What follows is a brief overview and critique of that work. Parameter notation for the most part follows that used by Hoppel. Much of Hoppel's work relies heavily on previous work of others which is appropriately referenced in his papers. For the most part these references are not specifically mentioned here.

There are five major papers for Hoppel's work. Hoppel (1977) provides the foundation for calculating the ion-aerosol attachment coefficients. Hoppel (1985) introduces (in his work) the time-dependent ion-aerosol balance equations and shows some example solutions. Hoppel and Frick (1986) give probably the most complete overall description of the aerosol charging problem. This paper reiterates most of the content of Hoppel (1977) and includes tables of attachment coefficients for typical tropospheric ions at normal temperature and pressure. It also demonstrates several solutions to the population balance equations including possible aerosol-aerosol interaction phenomena. Hoppel and Frick (1989) show probably the best test of the attachment coefficient theory against the experimental ultrafine unipolar aerosol charging data of Pui, Fruin and McMurry (1988). Some information about the sensitivity of calculated attachment coefficients to ion properties is provided. Hoppel and Frick (1990) treat the time-dependent ion-aerosol balance equations in depth, particularly with regard to the nonequilibrium nature of charge distributions from neutralizers. Several solutions are shown for different neutralizer configurations. The appendix provides a brief review of the problems involved in calculating attachment coefficients particularly with regard to the uncertainty in determining ion properties. Note is made of an improvement in the three-body trapping calculation, and tables are included of attachment coefficients for "typical" neutralizer ions at normal temperature and pressure. The reader is cautioned that there are many

typographical errors in the equations of these papers of which only a fraction have been discovered and noted.

POPULATION BALANCE EQUATIONS

The first (last) step in defining the aerosol charge distribution calculation is the system of time-dependent ion-aerosol population balance equations. Each equation equates the time derivative of a particular species to a sum of terms describing the birth and death processes for that species.

There is one equation each for positive and negative ions. Each ion equation has a generation/birth term (usually from radiation), an ion-ion recombination/death term, and death terms associated with each possible charge state of an aerosol particle. There may also be death terms associated with losses to containment surfaces. If more than one distinct ion species for a given polarity is considered (*e.g.* negative ions and free electrons), then there is one equation for each species and corresponding additional birth/death terms in all equations. Unless otherwise noted, the following discussion assumes there is only one distinct ion species of each polarity.

There is one equation for each of the possible charge states (k,i) of an aerosol particle. The series of charge states is generally truncated when the probability of achieving such a state becomes insignificant. Each equation has two birth terms corresponding to ion attachment to particles (of the same size) in adjacent charge states and two death terms corresponding to ion attachment to particles in the given charge state. Aerosol coagulation is generally ignored. For a polydisperse aerosol modeled as a set of discrete size classes, there is a set of balance equations for each size class and the ion equations have a death term associated with each possible charge state and size class of an aerosol particle. For a polydisperse aerosol modeled as a continuum, there is one size-dependent aerosol equation for each charge state and the ion-aerosol death terms in the ion equations become integrals over particular size.

In addition to the time derivative equations there may be conservation equations for charge and/or total particles of a given size. These are generally not all independent so that one or more may be eliminated. In the general case, the remaining system of equations must be solved simultaneously. In some cases, the ion concentrations may be treated as known in which case the ion time derivative equations are no longer required and the set of equations for each aerosol size may be solved independently of other sizes. This is the case when the ion-aerosol death terms in the ion equations are small with respect to the ion-ion recombination/death term. The ion equations can then be solved independently of the aerosol component to obtain the ion concentrations. In the case where ion generation is by radiation and the only significant death mechanism is by ion recombination then ion birth and death is always in pairs and the positive and negative ion concentrations must be equal (assuming there is no external field to separate the ions). Alternatively, the ion concentrations might be obtained by direct measurement. When steady-state conditions hold (time derivatives equal to zero) then the aerosol equations depend only on the ratio of positive and negative ion concentrations and absolute ion concentrations are not required. If ion birth and death are by radiation and recombination alone, then the ion concentration ratio is necessarily 1 and the ion equations need not be solved at all.

In most ambient stratospheric situations the total aerosol concentration is likely to be low enough that ion-aerosol interactions can be neglected in the ion balance equations. It is also likely that the steady-state solution may be used. If both conditions hold and a

neutralizer is not used before the DMA, then the ion concentration ratio is 1 and only the aerosol equations need be solved as indicated above. This may not be the case for the High Speed Research Program. It depends on the rate and extent of dilution of the aircraft exhaust. This also determines whether or not aerosol coagulation may be neglected in the charging equations. The relative magnitudes of the various birth/death terms in the charging equations cannot be determined until the attachment coefficients have been determined.

ATTACHMENT COEFFICIENTS

The next step in the aerosol charge distribution calculation is to determine the coefficients of the birth/death terms in the balance equations. If the ion equations are needed then knowledge of the ion generation rate, the ion recombination coefficient and the ion-aerosol attachment coefficients is required. The particle equations require only the ion-aerosol attachment coefficients.

The ion birth term is a single number, q, indicating the ion generation rate per unit volume. The natural ion generation rate in the stratosphere depends on pressure (altitude), temperature (?), solar zenith angle and perhaps other factors. In a radioactive neutralizer, the ion generation rate depends on pressure, temperature (?), source strength and type, distance from the source and perhaps other factors. The ion recombination/death term is the product of the ion recombination coefficient, α, and the positive and negative ion concentrations. The ion recombination coefficient depends on pressure, temperature and gas composition through the ion properties of mass and mobility. (Ion properties are discussed in more detail below.) There appears to be no theory available which can accurately predict the ion recombination coefficient from mass and mobility. The recombination rate must therefore be inferred from measurements (*e.g.* of generation rate and steady-state ion concentrations). If ion-aerosol interactions in the ion balance equations can be neglected, then the ion balance equations need not be solved but instead the ion concentrations may be measured. If steady-state conditions hold, then only the ion concentration ratio is needed. It is not clear that the temperature and/or pressure dependence of any of these ion variables can be accurately predicted. If not, measurements of ion concentrations (or whatever) would have to be obtained over the entire range of expected sampling conditions.

The ion-aerosol birth/death terms are each a product of an attachment coefficient, an ion concentration and a particle concentration. The ion-aerosol attachment coefficient, $\beta_{ji}^{(k)}(D_p)$, is the flux of ions of polarity j to a particle of diameter D_p carrying k charges of polarity i normalized to unit ion concentration. The ion-aerosol attachment coefficient depends on ion mass and mobility and on particle size, charge level, relative polarity and dielectric constant (see *e.g.* Pui, Fruin and McMurry, 1988). Besides indirect dependence through the above parameters, it also depends directly on temperature and mean molecular mass of the gas. If three-body ion trapping is important, then the ion recombination coefficient is required to estimate the ion-aerosol trapping distance.

The theory for calculating an ion-aerosol attachment coefficient is rather complicated. The Fuchs' (1963) limiting sphere approach has been generally successful in the transition regime. The exact radius of the limiting sphere varies from author to author but is generally on the order of one ion mean free path greater than the particle radius. Outside this sphere ion movement is treated in the continuum regime accounting for diffusion and electrical forces due to the image charge as well as the net charge on the particle. Inside the limiting sphere the ion is treated in the free molecule regime, *i.e.* in free flight within the imposed electric field. The fraction of ions entering the limiting

sphere which are actually captured by the particle must be calculated. This fraction and the exact location of the limiting sphere is where a large measure of the uncertainty in the overall calculation arises.

For pure coulombic attraction or repulsion, the ion is captured if and only if its trajectory takes it to the actual particle surface. For pure image charge there is a critical impact parameter and minimum apse (point of closest approach) for the possible ion trajectories. Ion trajectories with greater impact parameters approach the particle, pass through an apse and recede. Ion trajectories with lesser impact parameters have no apse and ultimately spiral in to the particle surface. The fraction of ions captured by the particle can be calculated analytically in either case. A numerical solution is required when there is both a net charge and an image charge. The calculation is further complicated if a distribution of ion velocities is considered at the limiting sphere. Following Keefe *et al.* (1968), Hoppel (1977) assumed a Maxwellian velocity distribution. However, the ions are being accelerated in the electric field of the particle. The resulting velocity bias built up by an ion between collisions with neutral gas molecules persists to some extent after a single collision due to the generally greater mass of the ion. There may thus be an accumulated velocity bias of the ions at the limiting sphere which is not accounted for. Integration over the velocity distribution to obtain the captured ion fraction can be carried out analytically for the pure coulombic and image potentials with Maxwellian velocity distribution but numerical solution is required in other cases. Using the numerical results of Keefe *et al.* (1968), Hoppel developed an approximation which appears to work satisfactorily at normal temperature and pressure. Its accuracy at reduced pressure and temperature is not easily extrapolated.

In the limit of very small particles, the ion-aerosol attachment coefficient must approach the ion recombination coefficient. One problem here is that the theory for ion-aerosol attachment generally treats the particle as stationary and only the ion moves. In the limit, the particle mass approaches the same order as the ion mass and both must be considered mobile. Hoppel (1977) notes that there are compensating effects in the theory which tend to cancel out this error. The other problem is that the main mechanism for ion recombination is three-body trapping. An ion approaching another ion of opposite polarity gains kinetic energy as it falls into the potential well of the attractive electric field. Collisions with neutral gas molecules tend to strip it of this excess kinetic energy until its total energy (kinetic + potential) becomes negative. At this point it no longer has enough kinetic energy to escape the potential well and the ions are trapped in orbit around each other. Further collisions modify this orbit until one ion achieves escape velocity by chance (presumably low probability), the ions collide or an electron penetrates the potential barrier between the two. It is necessary then to determine the fraction of ions which become trapped in orbit around a particle due to collision with one or more neutral air molecules.

Hoppel references Natanson (1960) with regard to his treatment of three-body trapping. In Hoppel's work a trapping distance is defined as that radius from the particle (electric field) center at which the ion accumulates a given amount of excess kinetic energy within a radial coordinate change equal to one mean free path. An ion entering at the Fuchs' limiting sphere is then considered captured if it is either captured directly by the electric forces (impact parameter less than the critical impact parameter described above) or if it collides with a neutral gas molecule within the three-body trapping distance. The calculation of fraction captured again relies on approximations concerning the velocity distribution and integration thereof.

Of greater concern though is the definition of trapping distance. The excess energy from which it is defined is obtained from a similar definition of the ion-ion trapping

distance. The ion-ion trapping distance is obtained from a measured value of the ion recombination coefficient using an equation of Natanson relating these two parameters. Since the analysis only looks at the excess kinetic energy accumulated in one mean free path length it appears that it ignores the accumulated loss of total energy which should be the relevant energy level to consider. It also ignores once again the persistence of velocity (hence, also excess kinetic energy) of the larger mass ion. In addition, Hoppel's definition of trapping distance from excess kinetic energy does not account for the random distribution of ion impact parameters.

Attempts to calculate three-body trapping distances directly from theory have not produced accurate results. Hoppel cites Brueckner (1964) as an example and uses his work to deduce the dependence of the ion-ion trapping distance on the ion/neutral gas molecule mass ratio. However, Brueckner not only failed miserably in predicting the magnitude of the trapping distance, but he also failed to weight his integrations over possible collision orientations by the probability of a collision which is proportional to the relative velocity of the colliding ion and neutral molecule.

[Consequently, from what I have read to date (which does not include Natanson's work nor any other primary reference on three-body trapping), calculations of three-body trapping distances seem rather questionable whether they are directly from theory or rely on measurements of ion recombination coefficients.]

Figure 3 in Hoppel (1977) and Figure 4 in Hoppel and Frick (1986) indicate that three-body trapping is only important for particles smaller than a few hundredths of a micron in radius at normal temperature and pressure. An equation in Hoppel and Frick (1986) (p. 12) gives dependence of trapping distance, d, on mean free path, λ, as $d \propto \lambda[(1+5e^2/3kT\lambda)^{1/2}-1]$ (attributed to Natanson). As pressure, p, is reduced, d goes up far more slowly than λ which is inversely proportional to p. The probability of collision with a neutral gas molecule within the trapping distance should go roughly as $1-\exp(-2d/\lambda)$ which should therefore decrease as pressure decreases. One would reason then, as did Hoppel (private communication), that three-body trapping decreases in importance at higher altitudes and reduced pressures and temperatures. Changes in d due to the temperature dependence should be of lesser magnitude than those due to the pressure dependence. Thus, if one is willing to accept the theoretical basis of three-body trapping, it may be possible to ignore the effects of three-body trapping within the flight range of the ER–2 for particles larger than a few hundredths of a micron.

Still of some concern is the exact location of the Fuchs' limiting sphere. Fuchs himself chose the average radius attained by ions traveling a distance of one mean free path in a random outward direction from the surface of the particle (Hoppel and Frick, 1986, Eq. 16). The displacement of this sphere from the particle surface is less than one mean free path. ($s=2\lambda/3$ for $\lambda<<a$ and $s=\lambda-a/3$ for $\lambda>>a$ where s is the displacement, λ is the mean free path and a is the particle radius.) Hoppel chooses the limiting sphere to be one mean free path from the image capture radius (minimum apse), Δ, or from the trapping distance, d, whichever is greater. The sensitivity of the overall calculation of ion-aerosol attachment coefficient to this variation is unknown.

ION PROPERTIES

The last step in the aerosol charge distribution calculation is to obtain the necessary ion properties. The properties needed are the mass, electrical mobility, diffusivity, mean thermal speed, and mean free path. Using relations cited in Hoppel and Frick (1986) and Pui, Fruin and McMurry (1988), the mean thermal speed can be calculated from mass and

the diffusivity from mobility at a given temperature. The diffusivity is proportional to mean free path, mean thermal speed and $(1+m/M)^{1/2}$ where m and M are the masses of the ion and neutral gas molecule, respectively. The constant of proportionality varies by slightly more than the square root of 2 according to whether one uses the equation of Loeb (Hoppel and Frick, 1986) or that of Kennard (Pui, Fruin and McMurry, 1988). Using either of these expressions, the mean free path can be obtained from the ion mass and mobility and the neutral gas molecule mass. The presence of the factor containing the mass ratio indicates that this represents a collision-free path and not a persistence path. As noted above, there are points in the theory where the persistence path might seem more appropriate. A persistence path can be obtained from the Loeb or Kennard expressions by omitting the mass ratio factor. For m=200 amu and M=29 amu the persistence path is larger than the collision-free path by a factor of 2.8.

Hoppel and Frick (1989) indicate that the calculation of attachment coefficient is relatively insensitive to the choice of using the Loeb or Kennard expression. Though switching to the persistence path is a somewhat greater variation, the calculation may be relatively insensitive to this as well. Similarly, one might expect little variation due to the various choices of the location of the Fuchs' limiting sphere. A more careful sensitivity analysis is required to verify this.

The minimum required ion properties are thus mass and mobility for both positive and negative ions. Various investigators have developed empirical plots or expressions relating mass and mobility. See, for example, references cited in the Appendix of Hoppel and Frick (1990), in Adachi, Kousaka and Okuyama (1985) and in Wiedensohler, Lütkemeier, Feldpausch and Helsper (1986). It is not clear how much confidence can be put in these expressions for the ER–2 application.

Measurements indicate that a range of properties is to be expected for each ion polarity corresponding to the range of possible molecules which may be incorporated in an ion. Ions also undergo evolution on several time scales as mentioned in the Appendix of Hoppel and Frick (1990). Thus, ions produced in a neutralizer used on the ER–2 are likely to be significantly different from ambient stratospheric ions. In either case it is possible to treat each distinct ion species individually in the population balance equations. This would be quite complicated and the available data on ion properties is probably insufficient to support such an analysis. Most investigators have chosen to use a single set of average ion properties for each polarity or even the same set for both polarities though the latter option is not recommended. This approach appears to be generally successful, but the error incurred is likely to increase as the range of ion properties increases. Wiedensohler and Fissan (1988) attempted to account for a second negative ion species – free electrons – in their work with ultrapure gases. It seems unlikely that there will be a significant concentration of free electrons in any charging situation imagined for an ER–2 based DMA but this should be considered. (See also O'Hara *et al.*, 1989.)

The papers mentioned in this section provide a number of references which should provide a good starting point for resolving the problem of determining ion properties. A few of these references have been already obtained and are listed under ion references.

CONCLUSIONS

Overall, the problem of aerosol charging for a DMA operated in the stratosphere may range from intractable to reasonable. It depends on the measurement conditions, the charging process used, availability of ion property data, and a sensitivity analysis of the charging theory.

It is recommended that the natural charge state of the aerosol be used. If an artificial charger is used, either a radioactive bipolar charger or a corona discharge unipolar charger, the charging process probably cannot be considered steady-state (Hoppel and Frick, 1990). There will be significant wall losses for the ions which will perturb the ion concentration ratio in a bipolar charger. There is probably far less data on artificially produced ions under stratospheric conditions than naturally occurring ones. The aerosol charge distribution from an artificial charger is likely to be a far stronger function of altitude than the naturally occurring charge distribution.

If the naturally occurring charge distribution can be considered steady-state and if the only significant ion birth and death processes are radiation and recombination, then the aerosol balance equations are relatively easy to solve. If three-body ion trapping can be neglected, then the ion-aerosol attachment coefficients can be carried out with a reasonable degree of confidence (subject to a sensitivity analysis). If all of the above conditions are met, the ion generation rate and recombination coefficient are not needed. All that is required then are ion masses and mobilities. The question remains as to what degree of confidence these may be predicted from the literature.

The conditions stated in the previous paragraph may not be satisfied when measuring supersonic transport exhaust. There may also be problems in measuring aerosols that have been in the dark for a long period. (Does the ion generation rate drop significantly in the dark?) If any of these conditions is not met, the complexity of the calculations increases and more data is required from the literature – data that may be more difficult to find and less reliable than the ion masses and mobilities. In this case, our confidence in the calculated aerosol charge distribution is likely to drop dramatically.

Appendix 3

Evaluation of Diffusion Batteries
for Stratospheric Aerosol Measurements

Diffusion batteries have the potential to be used to measure the size distributions of submicron particles in the stratosphere. This report presents the results of a feasibility study of this application of diffusion batteries.

A diffusion battery is device used to separate particles on the basis of their diffusional mobility. Particles are pulled through a "battery" of screens or tubes. Particles of a given size have a known probability of striking the battery matrix. This probability is higher for smaller particles (with higher diffusion coefficients) than for larger particles (with lower diffusion coefficients). By varying the flowrate and/or the number of screens or tubes, particles of different sizes can be selected to penetrate through the battery to reach a counting device (usually a condensation nuclei counter). The controlling parameter in diffusion battery performance is the inverse Peclet number, ϕ. For a tube-type diffusion battery, ϕ is defined (e.g., Brown et al., 1984) as

$$\phi = N_c \pi D^* L_c Q^{-1},$$

where Nc is the number of tubes in the diffusion battery, D* the diffusion coefficient, Lc the length of the tubes, and Q the volumetric flowrate. Particle diameter enters the formula through the diffusion coefficient, given as

$$D^* = \frac{kT}{3\pi\eta D_p}\left[1 + \frac{2.512\lambda}{D_p} + \frac{0.87\lambda}{D_p}\exp\left(\frac{-0.44D_p}{\lambda}\right)\right],$$

where k is Boltzmann's constant, T the temperature, η the viscosity of the fluid (air), l the mean free path of the fluid and D_p the diameter of the particle. The experimentally-determined efficiency of a particle penetrating a tube diffusion battery is given by (Brown et al., 1984)

$$\zeta = 0.819\exp(-3.65\Phi) + 0.097\exp(-22.3\Phi) \qquad [\Phi \geq 0.04] \quad \text{and}$$

$$\zeta = 1 - 2.56\Phi^{2/3} + 1.2\Phi + 0.177\Phi^{4/3} \qquad [\Phi < 0.04].$$

Measurements are obtained from the diffusion battery by selecting a "stage", a combination of flowrate, number of capillaries and capillary length. The number of particles penetrating each stage is then measured. These numbers (with error) and a knowledge of the penetration efficiency as a function of size (also with error due to the measurement of airflow) for each stage are used to extract the actual particle size distribution. The aerosol size distribution is assumed to remain constant while the number

concentration of particles penetrating each stage of the battery is measured. If a single CNC is used to cycle through each stage, obtaining statistically reasonable counts may take several minutes to tens of minutes at stratospheric concentrations.

A diffusion battery using commercially available glass capillary array filters has been modelled. The particle penetration efficiency for an ambient pressure of 50 mb at an instrument temperature of 273 K has been calculated as a function of particle diameter for each stage of the battery. These efficiencies are shown in Figure 2. The key feature of the penetration efficiency curves is the extremely broad nature of the response function for each stage of the battery. The measured response--the number concentration of particles penetrating each stage--is a convolution of the particle size distribution and these curves of particle penetration efficiency:

$$C_j = \int_{D_1}^{D_2} \zeta_j(D)\, N(D)\, dD, \qquad (3.1)$$

where C_j is the concentration of particles penetrating stage j of the diffusion battery, ζ_j the penetration efficiency of particles of size D penetrating stage j, N the concentration of particles of size D in the aerosol, and D_1 and D_2 the minimum and maximum particle diameters detectable with the CNC. Recovering the particle size distribution from the measurements C_j and known response functions $\zeta_j(D)$ involves inverting the integral to recover N(D). Unfortunately, for any given set of measurements C_j, an infinity of possible solutions exist that satisfy(3.1). Additionally, because the problem is extremely ill-posed, small errors in measurements can lead to very large errors in the inverted size distribution using traditional matrix inversion techniques. For most applications, the greatest difficulty in using diffusion batteries involves this inversion process. Because this process is the limiting factor in using diffusion battery data for stratospheric aerosol size distribution measurements, considerable effort was expended in examining various techniques.

The aerosol literature is full of techniques for solving the inversion problem. Most telling is that no single procedure has been universally accepted, and papers extolling new inversion techniques for diffusion batteries continue to appear. For this study, two new techniques for inverting diffusion battery data have been examined. The first of these, the Extreme Value Estimation (EVE) procedure, has been developed by P. Paatero of the University of Helsinki (Paatero, 1990). This technique does not attempt to find a single, "correct" size distribution, based on the argument that any size distribution that is consistent with the integral equation is valid. Instead, the EVE technique uses matrix inversion techniques to finds a solution set, limited to non-zero values, that is consistent with the measurements and their errors. The EVE program, which is commercially available from Dr. Paatero, was purchased for the purpose of this study. The source code for the software is not available.

The EVE program was used to invert a number of modelled size distributions. For modelled stratospheric measurements, the errors in the measurements due solely to counting statistics were sufficiently large to render the results essentially meaningless. The

deconvoluted family of size distributions that satisfied the equations within the estimated errors were broad enough to prevent reasonable determination of either the mean size or the geometric standard deviation of a simple lognormal, monomodal distribution.

An alternative method, the maximum entropy (MAXENT) technique, is based on the argument that the "best" solution of the particle size distribution is that containing the least "information content" in the language of information theory (Yee, 1989). The solution with the least information content is the simplest and smoothest of the possible solutions; it has no extraneous information beyond that warranted by the measurements. This concept can be expressed mathematically by the Shannon-Jaynes entropy equation,

$$H(n) = \int_{D_1}^{D_2} n(D)\ln[n(D)]dD,$$

where H(n) is the Shannon-Jaynes entropy, and n(D) the normalized particle size distribution function (i.e., the particle probalility distribution) such that $\int_{D_1}^{D_2} n(D)dD=1$. The MAXENT algorithm searches for n(D) that satisfies Eqn. 3.1 and that maximizes H(n). This method requires no *a priori, ad hoc* assumptions about the expected particle size distribution, as do most other inversion techniques, and produces a single size distribution by introducing the rational and valid constraint of maximum entropy.

The MAXENT algorithm was obtained from Dr. E. Yee of the Canadian Defence Research Establishment. Again, the source code was not made available. As before, a number of modelled diffusion battery measurements based on a known particle size distribution function were used as input to the inversion algorithm. Measurement errors were also used as input, although the penetration functions were assumed to be perfectly known (no allowance was made for errors in flow measurement). The MAXENT algorithm showed excellent potential by correctly recovering some of the input size distributions with very good accuracy when measurement errors were small. However, the algorithm was inherently unstable; tests using realistic particle size distributions with realistic errors did not recover any of the input distributions and instead oscillated wildly. These failures may be in part a product of numeric difficulties in the complex algorithm to solve the maximum entropy equation. Until these limitations are reduced, the algorithm is of little use when realistic measurement errors are introduced.

Conclusions

Diffusion batteries coupled with CNCs show some potential for estimating the size distribution of stratospheric particles. The technique is severly limited by the lack of robust algorithms for retrieving data with measurement errors. The MAXENT method shows some potential when measurement errors are small. By artificially introducing small errors into the MAXENT program, some qualitative information on the mean particle size may be obtained, although the substantial errors in the details of the retrieved size

distribution may result. Diffusion batteries cannot now be recommended for measurements of the stratospheric particle size distribution.

References

Brown, K. E., J. Beyer and J. W. Gentry, Calibration and design of diffusion batteries for ultrafine aerosols, *J. Aerosol Sci.*, **15**, 133-145, 1984.

Paatero, P., The extreme value estimation deconvolution method with applications in aerosol research, *Report Series in Physics HU-P-250*, University of Helsinki, Dept. of Physics, Siltavuorenpenger 20D, SF-00170 Helsinki, Finland, ISBN 951-45-4914-7, 41 pp., 1990.

Yee, E., On the interpretation of diffusion battery data, *J. Aerosol Sci.*, **20**, 797-811, 1989.